

Scanner-Based Capillary Stamping

Peilong Hou,* Ravi Kumar,* Bastian Oberleiter, Richard Kohns, Dirk Enke, Uwe Beginn, Harald Fuchs, Michael Hirtz,* and Martin Steinhart*

Classical microcontact printing and polymer pen lithography (PPL) involve ink transfer to substrates using solid elastomeric stamps. Ink depletion thus limits the number of successive stamping steps without reinking. Porous stamps developed to overcome this limitation are used only for manual proof-of-principle experiments. Here, porous composite stamps for scanner-based capillary stamping (SCS) that can be mounted on automated printing devices designed for PPL are developed. Porous SCS composite stamps consist of a rigid controlled porous silica glass (CPG) layer and a porous polymeric stamping layer. The latter can be topographically structured with contact elements by replication molding. The mechanical stabilization by the CPG layer ensures that the contact elements are coplanar. SCS allows automated, continuous, high-throughput patterning enabled by ink supply through the porous SCS composite stamps. Even after more than 800 consecutive stamp-substrate contacts without reinking (the porous SCS composite stamps themselves are used as ink reservoirs), ink microdroplets are deposited without deterioration of the pattern quality. However, SCS also allows supply of additional ink during ongoing stamping operations through the pore systems of the porous SCS composite stamps. SCS can easily be adapted for multi-ink patterning and may pave the way for further upscaling of contact lithography.

1. Introduction

Chemical and/or topographical patterning of substrates by contact lithography has been the focus of significant research efforts for more than two decades. Serial scanning probe lithography allows pixel-by-pixel generation of arbitrary patterns on the substrates.^[1] Modified scanning probe lithography configurations enable continuous fluidic ink supply to cantilever tips^[2] similar as in the case of micropipetting techniques.^[3] However, limited throughput and the limited sizes of the areas that can be patterned are inherent drawbacks of serial scanning probe lithography. Parallel high-throughput patterning of large substrate areas is possible by means of classical microcontact printing^[4] and its derivative polymer pen lithography (PPL).^[5] In these approaches, ink molecules adsorbed on the outer surfaces of solid elastomeric stamps are transferred to substrates by stamping. The capability to perform large numbers of successive stamping steps with short cycle times is a

prerequisite for the upscaling of soft lithography from benchtop experiments to automatized production processes. However, conventional microcontact printing suffers from ink depletion in the course of consecutive stamp-substrate contacts; hence, time-consuming interruptions of the printing operations for the readsorption of ink on the outer stamp surfaces are required to avoid deterioration of the quality of the stamped patterns. To overcome this drawback, stamps containing spongy continuous pore systems have been investigated because the continuous spongy pore systems enable continuous ink supply to the stamps' contact surfaces and can also be used as ink reservoirs themselves. For example, porous polymer stamps with pore sizes exceeding several 100 nm were produced by spinodal decomposition,^[6] and mesoporous silica stamps with pores having diameters of a few 10 nm by sol-gel chemistry.^[7] Porous block copolymer stamps with pore diameters of a few 10 nm were obtained by swelling-induced pore generation.^[8] In all these cases, contact surfaces topographically structured with contact elements also penetrated by the continuous spongy pore systems can be generated by replication molding during stamp preparation. Thus, ink transported through the continuous spongy pore system is deposited where the contact elements of the porous stamp touch the substrates to be patterned. So far, porous stamps have predominantly been used in manual proof-of-principle stamping experiments. Furthermore, porous

Dr. P. Hou, Prof. U. Beginn, Prof. M. Steinhart
 Institut für Chemie neuer Materialien and CellNanOS
 Universität Osnabrück
 Barbarastr. 7, Osnabrück 49076, Germany
 E-mail: peilong.hou@uos.de; martin.steinhart@uos.de

Dr. R. Kumar, Prof. H. Fuchs, Dr. M. Hirtz
 Institute of Nanotechnology (INT) and Karlsruhe
 Nano Micro Facility (KNMF)
 Karlsruhe Institute of Technology (KIT)
 Hermann-von-Helmholtz-Platz 1
 Eggenstein-Leopoldshafen 76344, Germany
 E-mail: ravi.kumar@kit.edu; michael.hirtz@kit.edu

B. Oberleiter, R. Kohns, Prof. D. Enke
 Institute of Chemical Technology
 Universität Leipzig
 Leipzig 04103, Germany

Prof. H. Fuchs
 Physical Institute and Center for Nanotechnology (CeNTech)
 University of Münster
 Münster 48149, Germany

 The ORCID identification number(s) for the author(s) of this article can be found under <https://doi.org/10.1002/adfm.202001531>.

© 2020 The Authors. Published by WILEY-VCH Verlag GmbH & Co. KGaA, Weinheim. This is an open access article under the terms of the Creative Commons Attribution License, which permits use, distribution and reproduction in any medium, provided the original work is properly cited.

DOI: 10.1002/adfm.202001531

stamps typically exhibit macroscopic waviness, which results from mechanical stress formed during stamp preparation and pore formation. If wavy stamps approach a substrate, at first an exposed portion of contact elements will touch the substrate, whereas other contact elements will contact the substrate only if the porous stamp is pressed against the substrate. Therefore, the pressure at the stamp–substrate interface and, as a result, the deposited patterns are locally different.

An optimized embodiment of contact lithography would comprise the automatized repetitive execution of stamping steps for parallel large-scale substrate patterning, as already realized for dip-pen lithography.^[5] However, interruptions of the stamping operations for reinking by ink adsorption on the stamp surface, each time followed by leveling procedures to align the stamp with the substrate, should be avoided. Stamps with spongy continuous pore systems appear to be ideal for the implementation of such a contact-lithographic process as they enable continuous fluidic ink supply to the stamps' contact surfaces. The objective of this work is the development of an automated large-area stamping procedure with stamps having spongy continuous pore systems, which is in the following referred to scanner-based capillary stamping (SCS). To this end, we specifically designed porous SCS composite stamps extending $5 \times 5 \text{ mm}^2$ that can be mounted on automated scanner-based positioning systems already established for PPL. The composite design ensured that the contact surfaces of the stamps' contact elements are coplanar on the macroscopic scale. Continuous ink supply from the continuous spongy pore systems of the porous SCS composite stamps to their contact surfaces enables continuous stamping without interruptions for reinking and without the need of controlled atmospheric conditions. Using the spongy continuous pore systems of porous SCS composite stamps as ink reservoir, we stamped 800 microdroplets per contact element by 800 successive stamp–substrate contacts under ambient conditions without reinking and without deterioration of the quality of the stamped pattern.

2. Results and Discussion

2.1. Design of Porous SCS Composite Stamps

The porous SCS composite stamps comprised porous polystyrene-*block*-poly(2-vinylpyridine) (PS-*b*-P2VP) stamping layers 1

tightly attached to $\approx 500 \text{ }\mu\text{m}$ thick, nondeformable controlled porous glass (CPG)^[9] layers 2. The CPG layers 2, which consisted of rigid silica scaffolds, mechanically stabilized the porous SCS composite stamps and prevented bending. The continuous pore systems of the CPG layers 2 were characterized by an average pore diameter of 102 nm, while the porosity of the GPG layers 2 amounted to 54%. To prepare the porous SCS composite stamps, we sandwiched molten asymmetric PS-*b*-P2VP containing P2VP minority domains in a PS matrix between the CPG layers 2 and silicon molds prepared by standard top-down lithography under a load of $\approx 2.75 \text{ bar}$ (Figure 1a). Since the CPG pores had oxidic walls with high surface energy, the PS-*b*-P2VP readily bonded to the CPG surfaces. The PS-*b*-P2VP surfaces opposite to the CPG/PS-*b*-P2VP interfaces were topographically patterned by replication molding against the silicon molds. The silicon molds had edge lengths of 10 mm and contained tetragonal lattices of pyramidal indentations with a nearest-neighbor distance of 200 μm . The edge length of the quadratic pyramid bases as well as the depths of the pyramids amounted to 50 μm . The native silica surfaces of the silicon molds were hydrophobically modified with trichloro(1*H*,1*H*,2*H*,2*H*-perfluorooctyl)silane (PFOTS). The silicon molds could thus easily be detached from the PS-*b*-P2VP bonded to the CPG layers 2. As a result, we obtained composites consisting of the CPG layers 2 and nonporous PS-*b*-P2VP layers with topographically patterned surfaces that were negative replicas of the silicon molds (Figure 1b). These composites were immersed into hot ethanol for swelling-induced pore formation in the PS-*b*-P2VP layers (Figure 1c).^[10] Following procedures reported elsewhere, we obtained continuous spongy pore systems characterized by a mean pore diameter of $\approx 40 \text{ nm}$, a specific surface area of $10 \text{ m}^2 \text{ g}^{-1}$, and a total pore volume of $0.05 \text{ cm}^3 \text{ g}^{-1}$.^[11] Hot ethanol is a solvent selective to P2VP so that osmotic pressure draws the ethanol in the P2VP minority domains. The volumes of the P2VP minority domains increase because the P2VP blocks tend to maximize favorable interactions with ethanol molecules by assuming stretched conformations. The swelling P2VP minority domains transform from discrete entities into a continuous network, while the glassy PS matrix undergoes morphology reconstruction to adapt to the increasing volume of the swelling P2VP domains. The swelling process is stopped if the ethanol is allowed to evaporate. Evaporation of the ethanol causes the entropic collapse of the expanded P2VP blocks that relax to random coils, while the glassy PS matrix fixates the

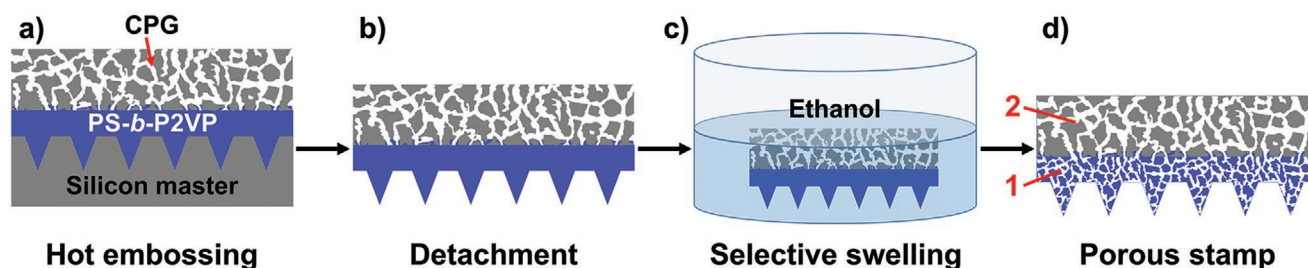


Figure 1. Preparation of porous SCS composite stamps. a) Molten PS-*b*-P2VP is sandwiched between a CPG layer and a hydrophobically modified silicon mold. b) After cooling to room temperature, the PS-*b*-P2VP/CPG composite is detached from the hydrophobically modified silicon mold and c) immersed into hot ethanol. d) Swelling-induced pore formation during exposure to hot ethanol results in the formation of a continuous spongy pore system in PS-*b*-P2VP stamping layer 1 tightly adhering to CPG layer 2.

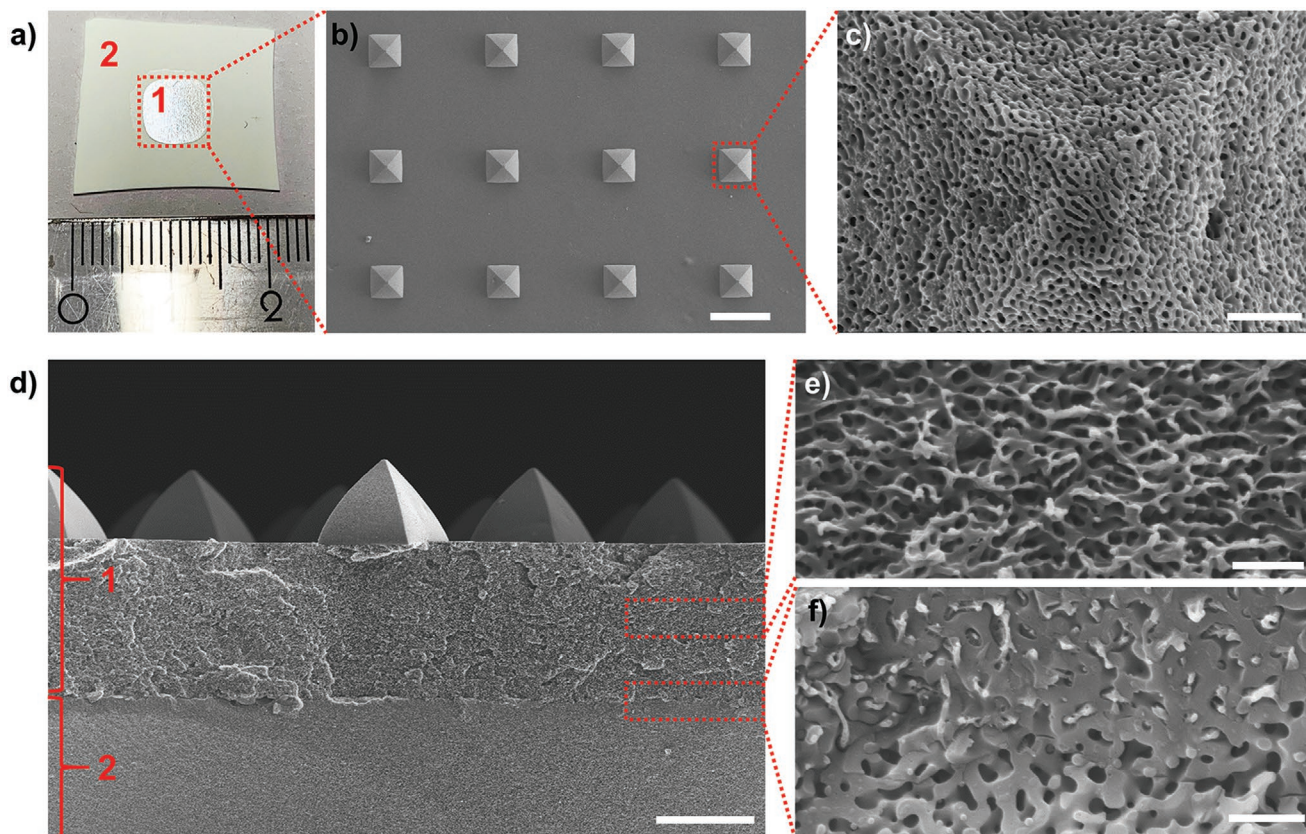


Figure 2. Porous SCS composite stamps. a) Photograph of a porous SCS composite stamp. The porous PS-*b*-P2VP stamping layer 1 extending ≈ 5 mm \times 5 mm is marked by the red dotted square. The size of the underlying CPG layer 2 is ≈ 20 mm \times 20 mm. b–f) Scanning electron microscope images. b) Top view of the contact surface of the porous PS-*b*-P2VP stamping layer 1 of a porous SCS composite stamp that is patterned with pyramidal contact elements. c) Detail showing a single pyramidal contact element. d) Cross-sectional view of a porous SCS composite stamp showing the porous PS-*b*-P2VP contact elements (top), the underlying porous PS-*b*-P2VP stamping layer 1 (center), and the CPG layer 2 (bottom). e) Detail of the porous PS-*b*-P2VP stamping layer 1. f) Detail showing a portion of the CPG layer 2 next to the CPG/PS-*b*-P2VP interface that is infiltrated with PS-*b*-P2VP. The lengths of the scale bars correspond to: (b) 100 μ m; (c) 1 μ m; (d) 50 μ m; (e, f) 500 nm.

reconstructed morphology. Thus, spongy continuous pore systems with walls consisting of coiled P2VP blocks form in lieu of the swollen P2VP domains. However, swelling-induced pore formation generates stress in the porous PS-*b*-P2VP stamping layers 1. While unsupported PS-*b*-P2VP stamping layers bend and develop macroscopic waviness, the CPG layers 2 mechanically stabilize the ≈ 80 μ m thick porous PS-*b*-P2VP stamping layers 1 of the porous SCS composite stamps (Figure 1d). The porous SCS composite stamps thus having coplanar contact elements extended 25 mm² (Figure 2a,b), while they were still completely penetrated by continuous spongy pore systems (Figure 2c–f). The pyramidal contact elements had flattened contact areas with edge lengths of ≈ 1 μ m at their tips (Figure S1, Supporting Information). The schematic representation of the porous SCS composite stamps in Figure 1 is somewhat simplified in that the PS-*b*-P2VP infiltrated the CPG layers 2 up to a depth of ≈ 3 μ m (Figure 2f). Hence, the CPG layers 2 and the porous PS-*b*-P2VP stamping layers 1 tightly adhered to each other, and no indications of delamination were apparent throughout the testing of the porous SCS composite stamps. Moreover, previous results^[12] suggest that swelling-induced pore generation also yields percolating pore systems even in local 2D confinement as it is imposed by the CPG pores.

2.2. Scanner-Based Capillary Stamping

For the SCS experiments, we used a commercial dip-pen nanolithography setup modified for PPL (Figure S2, Supporting Information). The device was controlled with an onboard software system that allows the design of arbitrary stamping patterns and the setting of parameters such as dwell times (i.e., the contact times between stamp and substrate). The porous SCS composite stamps were manually glued onto 2 mm thick custom-made metal stamp holders 3 extending 30 mm \times 80 mm with a square hole 4 extending 10 mm \times 10 mm (Figure S2a, Supporting Information, and Figure 3a–c). Thus, inking of porous SCS composite stamps is possible anytime in the course of their operation through hole 4 while mounted on a stamping device without the need to repeat time-consuming leveling procedures. Once leveled, an infinite number of stamping steps can be carried out without interruptions. Porous SCS composite stamps can, in principle, kept wet throughout their entire operational lifetime.

SCS stamping experiments were carried out using porous SCS composite stamps extending 0.5 cm \times 0.5 cm. At first, the porous SCS composite stamp was filled with oligo(1-decene), which we selected as model ink because of its low vapor pressure ($< 1 \times 10^{-7}$ torr at room temperature as specified by the

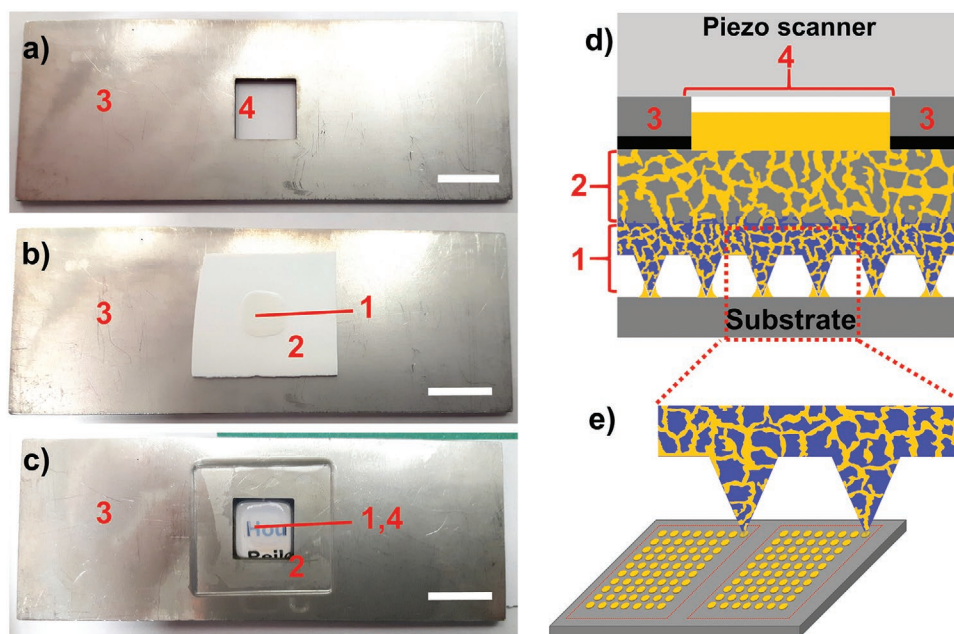


Figure 3. SCS stamping. a) Photograph of a stamp holder **3** with a central hole **4**, through which ink can be supplied even during ongoing SCS operations. b) Photograph of an empty porous SCS composite stamp consisting of a porous PS-*b*-P2VP stamping layer **1** located on a CPG layer **2** mounted on a stamp holder **3** in such a way that the central hole **4** is covered. c) Porous SCS composite stamp mounted on a stamp holder **3** after inking; the central hole **4** of the stamp holder can be seen through the transparent porous PS-*b*-P2VP stamping layer **1** and the CPG layer **2**. The lengths of the scale bars in panels (a)–(c) correspond to 1 cm. d) Schematic diagram of a cross section of a porous composite stamp. e) Schematic diagram of the SCS operation in which each contact element of a porous SCS composite stamp writes matrices of microdroplets by successive substrate contacts at different locations.

manufacturer). Typically, initial misalignment between stamp and substrate cannot be avoided. To compensate this misalignment, leveling of the porous SCS composite stamp was performed by adaptation of an optical leveling method reported previously.^[13] We used silicon wafers modified with hexamethyldisilazane (HMDS), thereafter referred to as HMDS-Si, as substrates for SCS. The contact angle of oligo(1-decene) on HMDS-Si amounted to $(49.6^\circ \pm 2.3^\circ)$ (Table S1, Supporting Information). After leveling, HMDS-Si was mounted onto the substrate stage of the lithography device. Following predefined SCS programs, the porous SCS composite stamp was brought into contact with the HMDS-Si substrate multiple times. The porous SCS composite stamp was slightly displaced laterally between two successive SCS cycles so that the contact elements contacted the substrate at slightly shifted positions (Figure 3d,e). For example, we generated arrays of matrices containing 8×10 oligo(1-decene) microdroplets; these arrays extended $5 \text{ mm} \times 5 \text{ mm}$ (Figure 4a; for a large-area optical microscopy image see Figure S3, Supporting Information)—corresponding to the extension of the PS-*b*-P2VP stamping layer **1**. Each 8×10 matrix of oligo(1-decene) microdroplets (Figure 4b) was written with one and the same contact element that contacted the HMDS-Si in 80 successive SCS steps without reinking. Between two successive SCS steps, the porous SCS composite stamp and thus the individual contact elements were displaced by $20 \mu\text{m}$, resulting in nearest-neighbor distances of $20 \mu\text{m}$ between adjacent oligo(1-decene) microdroplets. Hence, the distance between adjacent oligo(1-decene) microdroplets was one order of magnitude smaller than the distance between the tips of adjacent contact elements of the porous SCS composite stamp, which amounted to $200 \mu\text{m}$.

Here, we applied a dwell time of 10 s; the diameter of the oligo(1-decene) microdroplets amounted to $(7.78 \pm 1.40) \mu\text{m}$, and their height to $(1.92 \pm 0.16) \mu\text{m}$, as revealed by white-light interferometry (Figure S4, Supporting Information).

Elastomeric nonporous poly(dimethylsiloxane) (PDMS) stamps used for polymer pen lithography can hold absorbed volatile solvents for a few hours.^[14] In contrast, volatile solvents will rapidly evaporate from mesoporous materials^[15] and, consequently, from porous SCS composite stamps. However, this problem can be overcome by either triggered or continuous supply of ink or solvent through hole **4** of the stamp holder (Figure S2, Supporting Information, and Figure 3a) via CPG layer **2** to porous PS-*b*-P2VP stamping layer **1**. If non-volatile inks are used, the pore systems of the PS-*b*-P2VP stamping layers **1** and the CPG layers **2** may act themselves as long-term ink reservoirs. In the case of oligo(1-decene), ink-filled porous SCS composite stamps could even be reused with same ink load after several days. To exploratively evaluate how many successive SCS cycles can be performed without reinking, we carried out a SCS sequence in which one 8×10 matrix of oligo(1-decene) microdroplets per contact element was stamped on HMDS-Si and repeated this sequence on nine more HMDS-Si substrates. As a result, ten 8×10 matrices of oligo(1-decene) microdroplets—corresponding to 800 oligo(1-decene) microdroplets—were generated per contact element without reinking the porous SCS composite stamps. Figure 4c,d shows optical microscopy images of 8×10 matrices of oligo(1-decene) microdroplets on the tenth HMDS-Si substrate. The diameter of the oligo(1-decene) microdroplets amounted to $(7.20 \pm 1.33) \mu\text{m}$. Therefore, one

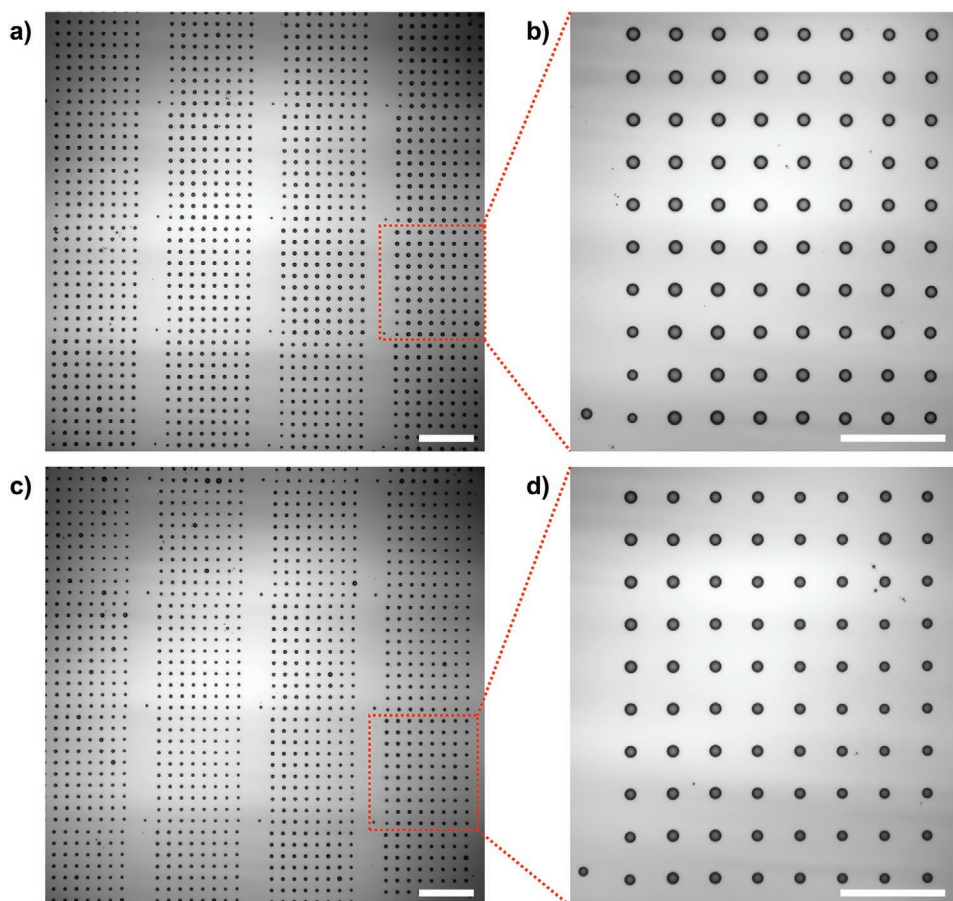


Figure 4. Optical microscopy images showing 8×10 matrices of oligo(1-decene) microdroplets formed by SCS on HMDS-Si with a dwell time of 10 s. Each 8×10 matrix was generated by 80 successive contacts between one single contact element of the porous SCS composite stamp and HMDS-Si. a,b) First substrate stamped after inking. c,d) Tenth substrate that was successively stamped without reinking the porous SCS composite stamp. The red dotted rectangles in panels (a) and (c) denote exemplary 8×10 matrices of microdroplets generated with one contact element. Panels (b) and (d) show exemplary 8×10 matrices of microdroplets generated with one contact element. The 8×10 matrix seen in panel (b) represents the stamping results of substrate contacts 1–80 and the 8×10 matrix seen in panel (d) the stamping results of substrate contacts 721–800 of a single contact element. In panels (a) and (c), the lengths of the scale bars correspond to $100 \mu\text{m}$. In panels (b) and (d), the lengths of the scale bars correspond to $50 \mu\text{m}$.

individual contact element of a porous SCS composite stamp can generate at least 800 microdroplets without reinking and without significant deterioration of the pattern quality. It is, of course, also possible to write arbitrary patterns instead of the 8×10 matrices displayed in Figure 4, as exemplarily shown in Figure S5 (Supporting Information).

In another set of experiments, we investigated the impact of the dwell time and the oligo(1-decene) contact angle on the counterpart substrates on size and shape of the deposited oligo(1-decene) microdroplets. In a first experiment, we stamped arrays of 4×8 matrices of oligo(1-decene) microdroplets onto HMDS-Si, i.e., each contact element of the porous SCS composite stamp stamped one 4×8 matrix by 32 successive contacts with HMDS-Si. For each of the four stamped columns, we varied the dwell time from 1 to 5 s to 10 to 20 s (Figure 5a,b). The average diameters of the oligo(1-decene) microdroplets amounted to $(4.0 \pm 0.6) \mu\text{m}$ for a dwell time of 1 s, to $(4.5 \pm 0.4) \mu\text{m}$ for a dwell time of 5 s, to $(5.9 \pm 0.8) \mu\text{m}$ for a dwell time of 10 s, and to $(6.4 \pm 0.7) \mu\text{m}$ for a dwell time of 20 s. Hence, with increasing dwell time a moderate increase in the oligo(1-decene) microdroplet diameter occurs. Next, we modified

the contact angle of oligo(1-decene) on the counterpart substrate by replacing HMDS with (3-aminopropyl)triethoxysilane (APTES). On silicon wafers modified with APTES (APTES-Si), oligo(1-decene) spreads (i.e., the contact angle is 0° , see Table S1, Supporting Information). As in the case of HMDS-Si, we stamped 4×8 matrices of oligo(1-decene) microdroplets onto APTES-Si and varied the dwell time for each column. For a dwell time of 1 s, the diameter of the oligo(1-decene) microdroplets amounted to $(16.9 \pm 0.6) \mu\text{m}$. However, for dwell times of 5, 10, and 20 s, the oligo(1-decene) microdroplets merged and formed microlines.

Since we focus on the problem of ink depletion in the course of successive stamping steps associated with the use of solid elastomeric stamps, we aimed at stamping large ink microdroplets even after 800 stamp–substrate contacts without reinking. Reductions of the feature sizes of the stamped structures should be straightforward by appropriate adaptations of the shape of the contact elements and/or the contact angles of the ink–substrate systems. Deposited structures with diameters in the 100 nm range consisting of nonvolatile ink components dissolved or dispersed in a volatile solvent may be accessible also.^[7a]

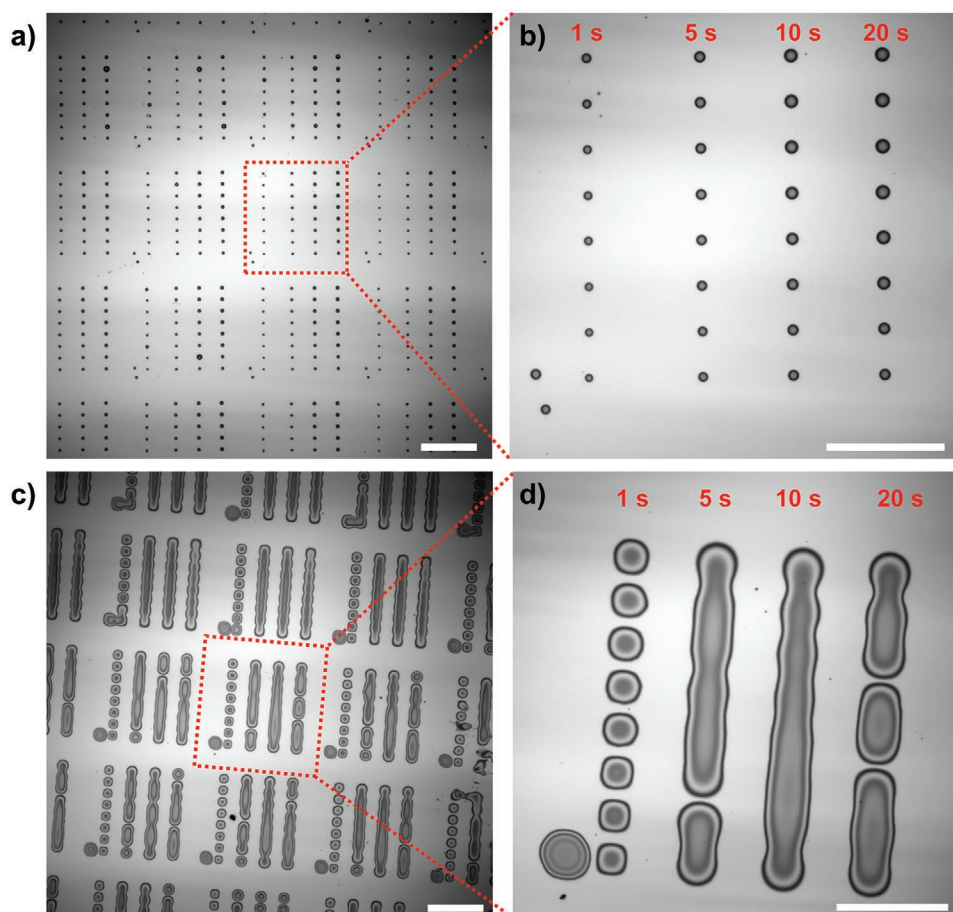


Figure 5. Optical microscopy images of 4×8 matrices of oligo(1-decene) microdroplets deposited with a single contact element and without reinking on Si wafers coated with a,b) HDMS and c,d) APTES. The spacing between the oligo(1-decene) microdroplets amounts to $40 \mu\text{m}$ in the x-direction and to $20 \mu\text{m}$ in the y-direction. For each of the four rows of a 4×8 matrix, a different dwell time was applied—from the left to the right 1, 5, 10, and 20 s. a,c) Large-area views; exemplary 4×8 oligo(1-decene) microdroplet arrays are marked by red dotted rectangles. b,d) Details showing exemplary 4×8 matrices. In panels (a) and (c), the lengths of the scale bars correspond to $100 \mu\text{m}$; in panels (b) and (d), the lengths of the scale bars correspond to $50 \mu\text{m}$.

2.3. Multi-Ink SCS

Multi-ink patterning or multiplexing involves the application and integration of more than one ink in an interdigitated

microscale pattern.^[16] In an exploratory activity, we evaluated a stamp configuration potentially allowing multiplexing SCS. We used 2 mm thick custom-made stamp holders **3** extending $30 \text{ mm} \times 80 \text{ mm}$ that contained two holes **4** extending

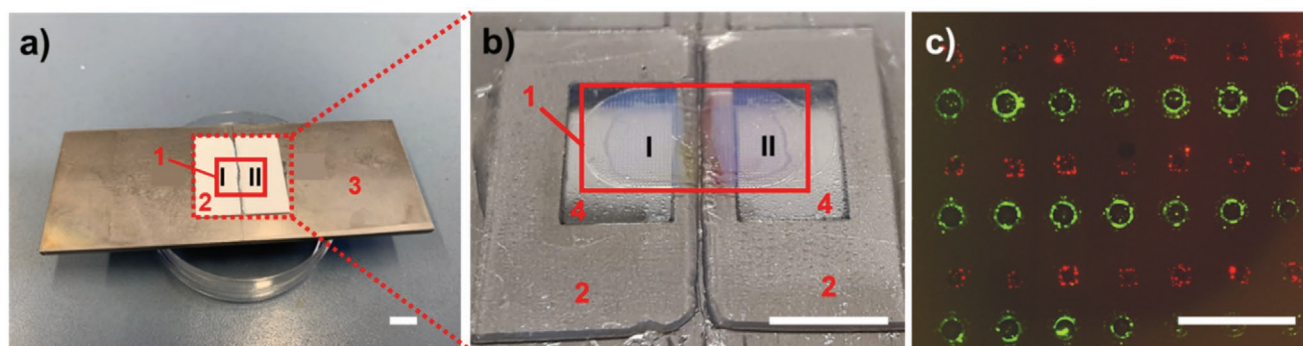


Figure 6. Multi-ink SCS. a,b) Photographs of a SCS configuration adapted for multiplexing prior to and after inking. The stamp holder **3** contains two holes **4** extending $5 \text{ mm} \times 10 \text{ mm}$. The holes are covered by two separated parts of a porous SCS composite stamp (denoted by I and II) consisting of the PS-*b*-P2VP stamping layer **1** and the CPG layer **2**. Parts I and II can then be independently loaded with different inks (ink I and ink II) c) Fluorescence microscopy image showing a two-color pattern obtained by multi-ink SCS (corresponding bright field images are shown in Figure S7, Supporting Information). The lengths of the scale bars correspond to (a, b) 0.5 cm and (c) $200 \mu\text{m}$.

5 mm × 10 mm (Figure 6a,b and Figure S6, Supporting Information). The surfaces of the CPG layers 2 of the porous SCS composite stamps were glued onto the stamp holders 3 as described earlier. The porous SCS composite stamps were then cut into two separate parts (part I and part II) with a sharp knife. Each part consisted of a porous PS-*b*-P2VP stamping layer 1 patterned with an array of contact elements extending ≈0.5 cm × 0.4 cm located on the CPG layers 2 that in turn covered the holes 4 of the stamp holders 3. The contact surface of part I was coated with the dye 18:1 Liss Rhod PE showing fluorescence at a wavelength of 583 nm, and the contact surface of part II with the dye 18:1 PE CF showing fluorescence at a wavelength of 515 nm. Both dyes, which form phospholipid inverted micelles,^[17] were used as marker molecules that were selected because of their compatibility with the test ink oligo(1-decene). Oligo(1-decene) was supplied to the surface of the CPG layers 2 through the two holes 4 in stamp holder 3. For the leveling of the porous SCS composite stamps, the method described earlier for single-ink SCS was applied. However, only one of the two separated parts was leveled assuming conformity of the other part. Hence, even after the leveling misalignment still existed to some extent. Multi-ink microdroplet patterns were stamped by repositioning the piezo-driven substrate stage in such a sequence that subpatterns of each particular ink were generated next to each other (Figure 6c). First, part I of the porous SCS composite stamp generated arrays of matrices containing 1 × 2 ink I microdroplets (by contacting the substrate once, then a second time after moving it by 100 μm in *x*-direction, dwell time 1–10 s depending on specific experiment). This results in bands of ink I microdroplets with a distance of 100 μm between ink I microdroplets within one band and 200 μm distance between two adjacent bands. Then, by moving the part II of the SCS stamp over the already formed arrays of microdroplets and aligning the contact elements with the empty substrate area between the bands of ink I microdroplets, intermediate bands of ink II microdroplets were generated, resulting in a two-color band pattern with 100 μm distanced microdroplets (Figure 6c). The fluorescent inverted-micellar dyes enriched at the outer rims of the otherwise fully formed microdroplets (Figure S7, Supporting Information)—likely because of convection patterns^[18] inside the microdroplets similar to the coffee-ring effect^[19] in faster-evaporating liquids. Because of the exploratory nature of multi-ink SCS, there is additional variance in the microdroplet size due to the implementation of printing position and dwell time by manual control of the lithography setup. In future developments, this can be automated as in PPL strategies^[16b,c] to achieve fully homogeneous patterning as shown for SCS in mono-ink patterning above.

3. Conclusions

Classical microcontact printing with solid elastomeric stamps suffers from ink depletion if several consecutive stamping steps are carried out without reinking. Spongy porous stamps may overcome these drawbacks but have, so far, only been used for manual proof-of-principle experiments. Scanner-based capillary stamping involves the incorporation of porous stamps into automated stamping systems already established for polymer

pen lithography. To this end, we have designed porous SCS composite stamps consisting of a porous polymeric stamping layer, which can be topographically patterned with contact elements by replication molding, and a rigid layer consisting of inorganic controlled porous glass. The CPG layers mechanically stabilizing the porous SCS composite stamps prevent bending and bulging so that a coplanar arrangement of the stamps' contact elements is ensured. The SCS design enables ink supply anytime during ongoing stamping operations to the backsides of the porous SCS composite stamps. The ink is then transported through the pore systems of the porous SCS composite stamps to the contact surfaces of the porous polymeric stamping layers. Porous SCS composite stamps can, in principle, kept wet during their entire operational lifetime. Especially if nonvolatile inks are stamped, the pore systems of the porous SCS composite stamps can be used as ink reservoirs. Using oligo(1-decene) as nonvolatile model ink, 800 ink microdroplets could be stamped successively with one single contact element by 800 successive substrate contacts without reinking and without deterioration of the pattern quality. Moreover, exploratory experiments revealed that SCS can be adapted for multi-ink patterning by multiplexing. Therefore, SCS may pave the way for further automatization and upscaling of contact lithography.

4. Experimental Section

Chemicals: Asymmetric PS-*b*-P2VP ($M_n(\text{PS}) = 101\,000\text{ g mol}^{-1}$; $M_n(\text{P2VP}) = 29\,000\text{ g mol}^{-1}$; $M_w/M_n(\text{PS-}b\text{-P2VP}) = 1.60$, volume fraction of P2VP 21%; bulk period 51 nm) was obtained from Polymer Source Inc., Canada. P2VP homopolymer ($M_w = 41\,000\text{ g mol}^{-1}$; $M_n = 37\,000\text{ g mol}^{-1}$; $M_w/M_n = 1.11$) was obtained from Sigma-Aldrich. HMDS was supplied by abcr GmbH. APTES and PFOTS were purchased from Sigma-Aldrich. Tetrahydrofuran (THF), hydrogen peroxide (30% H₂O₂), sulfuric acid (98% H₂SO₄), and ethanol were supplied by local manufacturers in the analytical grade.

Silicon Molds: Silicon molds were prepared as reported previously.^[5a] The surface of the silicon molds was topographically patterned with tetragonal lattices of pyramidal indentations with a nearest-neighbor distance of 200 μm. The edge length of the quadratic pyramid bases amounted to 50 μm. The depth of the pyramidal indentations also amounted to 50 μm. Before use, the surface of the silicon molds covered by native oxide was silanized with PFOTS. For this purpose, silicon molds were at first treated with a boiling mixture containing 98% H₂SO₄ and 30% H₂O₂ at a volume ratio of 7:3 for 30 min, followed by rinsing with deionized water and drying in an argon flow. Then, the silicon molds were kept under a vacuum at room temperature for 5 h in the presence of 0.2 mL PFOTS.

CPGs: CPG layers extending 2 cm × 2 cm with an average pore diameter of 102 nm, a thickness of 500 μm, and porosity of 54% were prepared by spinodal decomposition of alkali borosilicate glasses and subsequent leaching of the boron-rich phase following procedures reported elsewhere.^[9] The CPG layers were characterized by mercury intrusion porosimetry (MIP) carried out on a Pascal 140/440 porosimeter (Thermo Fisher Scientific, Waltham, MA) over a pressure range of 0.15–200 MPa (Figure S8, Supporting Information). Pore size distributions were derived from the MIP data with Pascal software according to the Washburn equation, setting the mercury contact angle to 141°; the measured pressure range corresponds to pore diameters between 14 nm and 10 μm.

Silicon Substrates: Silicon wafers (Part No. L14025) were obtained from Siebert Wafer GmbH, Aachen. To silanize the silicon wafers with HMDS or APTES, they were at first treated with a boiling mixture containing 98%

H₂SO₄ and 30% H₂O₂ at a volume ratio of 7:3 for 30 min, followed by rinsing with deionized water and drying in an argon flow. Then, the silicon wafers were heated for 5 h to 100 °C in the presence of 0.2 mL of the respective silane under ambient pressure. For further use, the silanized silicon wafers were cut into squares with an edge length of ≈1 cm.

Inks: For single-ink stamping, oligo(1-decene) (Inland 45 vacuum pump fluid; kinematic viscosity at 40 °C as specified by the manufacturer: 53 cSt; vapor pressure <1 × 10⁻⁷ torr) purchased from Inland Vacuum Industries (Churchville, NY) was used as ink. Size exclusion chromatography revealed the following values for the molecular mass of oligo(1-decene): $M_w = 490 \text{ g mol}^{-1}$; $M_n = 390 \text{ g mol}^{-1}$; $M_w/M_n = 1.26$. For multi-ink stamping, the fluorescently labeled phospholipids (18:1 Liss Rhod PE (full name: [1,2-dioleoyl-sn-glycero-3-phosphoethanolamine-N-(rhodamine rhodamine B sulfonyl) (ammonium salt)]) and 18:1 PE CF (full name: [1,2-dioleoyl-sn-glycero-3-phosphoethanolamine-N-(carboxy-fluorescein)]) supplied by Avanti Polar Lipids (USA) were used. Both dyes were applied as solutions in oligo(1-decene) containing 0.1 mg mL⁻¹ dye.

Fabrication of Porous SCS Composite Stamps: PS-*b*-P2VP films were prepared by dropping 50 μL (stamp for single-ink stamping) or 100 μL (stamp for multi-ink stamping) of a solution of 100 mg mL⁻¹ PS-*b*-P2VP in THF onto a silicon wafer extending 5 mm × 5 mm (stamp for single-ink stamping) or 10 mm × 5 mm (stamp for multi-ink stamping). After complete evaporation of the THF, the obtained PS-*b*-P2VP films were nondestructively detached by exposure to ethanol for 24 h at room temperature. Then, PS-*b*-P2VP films were sandwiched between CPG layers 2 and surface-modified silicon molds at 220 °C for 4 h under a vacuum while a load of ≈2.75 bar was applied. After cooling to room temperature at -1 K min⁻¹, the silicon molds were detached from the PS-*b*-P2VP by treatment with ethanol at room temperature for ≈30 min. For swelling-induced pore generation, PS-*b*-P2VP attached to CPG layers 2 was treated with ethanol at 60 °C for 4 h. Under the conditions applied here, spongy-continuous pore systems with a mean pore diameter of ≈40 nm, a specific surface area of 10 m² g⁻¹, and a total pore volume of 0.05 cm³ g⁻¹ formed.^[1]

Stamping Device Used for SCS: All stamping experiments were carried out with an NLP 2000 device (Nanoink Inc., USA) equipped with three encoded piezo-driven linear substrate stages displaceable in the X, Y, and Z directions as well as with an encoded goniometer stage (settings are referred to T_x and T_y), which can move 40 mm in the X and Y directions as well as 10 mm in the Z direction. The in-built camera system has a spatial resolution better than 1 μm and a digitally controlled halogen illumination system. The NLP 2000 device was controlled with an onboard software system that allows designing patterns and setting dwell times (i.e., the contact time between stamps and substrates).

Single-Ink Inking: 2 mm thick custom-made metal stamp holders 3 extending 30 mm × 80 mm with a square hole 4 extending 10 mm × 10 mm were used. The surfaces of the CPG layers 2 of the porous SCS composite stamps were glued onto the stamp holders 3 with a two-component epoxy resin adhesive (UHU, Germany) in such a way that the CPG layers 2 covered the holes 4 in the stamp holders 3. Then, stamp holders 3 were glued onto the bars of custom-made frame (Figure 3a-c and Figure S2a, Supporting Information) that were in turn mounted on the NLP 2000 device (Figure S2c, Supporting Information). For inking, 200 μL oligo(1-decene) was deposited into the holes 4 of the stamp holders 3. After a wait time of 2 h, the ink-soaked porous SCS composite stamps were fully transparent.

Multi-Ink Inking: For multi-ink stamping, 2 mm thick custom-made stamp holders 3 extending 30 mm × 80 mm that contained two holes 4 extending 5 mm × 10 mm (Figure 6a) were used. The surfaces of the CPG layers 2 of the porous SCS composite stamps were glued onto the stamp holders 3 as described earlier. The porous SCS composite stamps were then cut into two separate parts with a sharp knife in such a way that each part covered one of the holes 4 in the stamp holders 3. 20 μL portions of the ink solutions were deposited onto the contact surfaces of the porous PS-*b*-P2VP stamping layers 1 using an Eppendorf pipette. After a wait time of 1 h, the stamp holders 3 were mounted onto the NLP 2000 device. Then, 100 μL oligo(1-decene) was deposited onto each part of the porous SCS composite stamps through the two holes 4 in the

stamp holders 3 via the surface of the CPG layers 2. After a wait time of 2 h, the ink-soaked porous SCS composite stamps were fully transparent.

Leveling of the Porous SCS Composite Stamps: After inking, the porous SCS composite stamps were optically fully transparent (Figure 3c) so that the leveling procedure could be monitored by optical microscopy using objectives and a digital camera located atop of the CPG layer 2 away from the contact surface of PS-*b*-P2VP stamping layer 1. A silicon test substrate mounted on a substrate stage adjustable by a goniometer was brought into contact with the pyramid-shaped contact elements of the ink-filled porous SCS composite stamp. As soon as the substrate stage was about 100–200 μm away from the contact elements, shadows appeared due to the reflective nature of the silicon test substrate (Figure S9a, Supporting Information). When the contact elements contacted the substrate surface, circular ink microdroplets formed at the contact sites (Figure S9b, Supporting Information). In the course of the initial approach of the silicon test substrate toward the porous SCS composite stamp, the tips of some of the pyramid-shaped contact element touch the silicon test substrate harder than others, resulting in local variations of the sizes of the deposited ink microdroplets. To compensate for this, the substrate stage was stepwisely tilted about the two goniometer axes. For each goniometer setting, a stamping test was carried out, and the variance in microdroplet sizes was evaluated by visual inspection of the corresponding optical microscopy images. This procedure was repeated until the microdroplet size was uniform all over the silicon test substrate, indicating that the plane of the silicon substrate stage was parallel to the plane of the stamp. For the leveling of the porous SCS composite stamps for multi-ink stamping, a similar method was applied, but only one of the two separated parts was leveled assuming conformity of the other part. Small misalignments are still to be expected after the leveling.

General SCS Stamping Procedure: After leveling, HMDS-Si or APTES-Si were mounted onto the substrate stage of the NLP 2000 device and employed as substrates. The substrates were approached to the porous SCS composite stamps until the distance amounted to ≈100 μm. Then, the porous SCS composite stamps were further approached to the substrates in steps of 10 μm until contact was formed. Contact formation detected optically by the in-built camera was indicated by the formation of circular microdroplets at around the tips of the contact elements. After a predefined dwell time, the substrates were retracted by 50 μm, moved to the next set position, and brought in contact with the SCS stamps again for the next stamping step. This cycle was repeated multiple times until the predefined stamping program was completed. The general procedure for multi-ink stamping was an adaptation of a previously published approach.^[16b,c] Multi-ink microdroplet patterns were stamped by repositioning the piezo-driven substrate stage in such a sequence that subpatterns of each particular ink were generated next to each other (Figure 6c and Figure S7, Supporting Information). The initial offset between parts I and II of the SCS stamps was corrected by visual in situ alignment using the optical microscope attached to the NLP 2000 device.

Characterization: The molecular mass of oligo(1-decene) was determined by gel permeation chromatography using a Waters 2695 Separations Module and THF as solvent against PS as standard for external calibration.

Ink contact angles (Table S1, Supporting Information) were measured in the sessile drop mode at a humidity of 27% and a temperature of 23 °C using a drop shape analyzer DSA100 (Krüss, Germany). The volumes of the liquid droplets were 3 μL. All contact angle measurements for a specific sample type were repeated on six different samples. P2VP homopolymer films for the contact angle measurements were prepared by spin-coating a solution of 10 wt% P2VP in ethanol onto a silicon wafer at 1000 rpm, followed by drying in vacuum.

Scanning electron microscopy (SEM) investigations were carried out on a Zeiss Auriga microscope operated at an accelerating voltage of 5 kV. Prior to the SEM investigations, the samples were coated with an ≈5 nm thick iridium layer. The diameters of the microdroplets were determined using NIS-Elements imaging software by evaluating around 100 microdroplets per sample. White light interferometry was carried out on a ContourGT-K 3D Optical Microscope using Vision64 Operation and Analysis Software. Fluorescence microscopy images were acquired with

an upright fluorescence microscope (reflection mode, Eclipse 80i, Nikon Germany) equipped with a sensitive camera (Nikon DS-Qi2 camera from Nikon Germany), a broadband excitation light source (Intensilight, Nikon), a FITC filter set (B-2E/C, Nikon), and a Texas Red filter set (Y-2E/C, Nikon). For different colors, the fluorescence microscopy images were captured separately and then merged using NIS-Elements imaging software.

Supporting Information

Supporting Information is available from the Wiley Online Library or from the author.

Acknowledgements

P.H. and R.K. contributed equally to this work. The authors thank the European Research Council (ERC-CoG-2014, Project 646742 INCANA) for funding. This work was partly carried out with the support of the Karlsruhe Nano Micro Facility (KNMF, www.knmf.kit.edu), a Helmholtz Research Infrastructure at Karlsruhe Institute of Technology (KIT, www.kit.edu). The authors thank Richard Thelen (Institute of Microstructure Technology (IMT), Karlsruhe Institute of Technology (KIT)) for help with the white light interferometry measurements.

Conflict of Interest

The authors declare no conflict of interest.

Keywords

block copolymers, composite materials, microcontact printing, polymeric materials, porous materials

Received: February 18, 2020

Revised: March 23, 2020

Published online: April 26, 2020

- [1] a) R. D. Piner, J. Zhu, F. Xu, S. Hong, C. A. Mirkin, *Science* **1999**, *283*, 661; b) M. Jaschke, H.-J. Butt, *Langmuir* **1995**, *11*, 1061.
- [2] a) A. Meister, M. Liley, J. Brugger, R. Pugin, H. Heinzelmann, *Appl. Phys. Lett.* **2004**, *85*, 6260; b) S. Deladi, J. W. Berenschot, N. R. Tas, G. J. M. Krijnen, J. H. de Boer, M. J. de Boer, M. C. Elwenspoek, *J. Micromech. Microeng.* **2005**, *15*, 528; c) K.-H. Kim, N. Moldovan, H. D. Espinosa, *Small* **2005**, *1*, 632; d) A. Fang, E. Dujardin, T. Ondarcuhu, *Nano Lett.* **2006**, *6*, 2368.
- [3] K. T. Rodolfa, A. Bruckbauer, D. Zhou, A. I. Schevchuk, Y. E. Korchev, D. Klenerman, *Nano Lett.* **2006**, *6*, 252.
- [4] a) Y. Xia, G. M. Whitesides, *Annu. Rev. Mater. Sci.* **1998**, *28*, 153; b) D. Qin, Y. Xia, G. M. Whitesides, *Nat. Protoc.* **2010**, *5*, 491; c) A. Perl, D. N. Reinhoudt, J. Huskens, *Adv. Mater.* **2009**, *21*, 2257; d) T. Kaufmann, B. J. Ravoo, *Polym. Chem.* **2010**, *1*, 371.
- [5] a) F. Huo, Z. Zheng, G. Zheng, L. R. Giam, H. Zhang, C. A. Mirkin, *Science* **2008**, *321*, 1658; b) A. B. Braunschweig, F. Huo, C. A. Mirkin, *Nat. Chem.* **2009**, *1*, 353; c) C. Carbonell, A. B. Braunschweig, *Acc. Chem. Res.* **2017**, *50*, 190; d) G. Liu, M. Hirtz, H. Fuchs, Z. Zheng, *Small* **2019**, *15*, 1900564.
- [6] H. Xu, X. Y. Ling, J. van Bennekom, X. Duan, M. J. W. Ludden, D. N. Reinhoudt, M. Wessling, R. G. H. Lammertink, J. Huskens, *J. Am. Chem. Soc.* **2009**, *131*, 797.
- [7] a) M. Schmidt, M. Philippi, M. Münzner, J. M. Stangl, R. Wiczorek, W. Harneit, K. Müller-Buschbaum, D. Enke, M. Steinhart, *Adv. Funct. Mater.* **2018**, *28*, 1800700; b) M. Philippi, C. You, C. P. Richter, M. Schmidt, J. Thien, D. Liße, J. Wollschläger, J. Piehler, M. Steinhart, *RSC Adv.* **2019**, *9*, 24742.
- [8] a) L. Guo, M. Philippi, M. Steinhart, *Small* **2018**, *14*, 1801452; b) W. Han, E. Stepula, M. Philippi, S. Schlücker, M. Steinhart, *Nanoscale* **2018**, *10*, 20671.
- [9] D. Enke, F. Janowski, W. Schwieger, *Microporous Mesoporous Mater.* **2003**, *60*, 19.
- [10] a) Y. Wang, C. He, W. Xing, F. Li, L. Tong, Z. Chen, X. Liao, M. Steinhart, *Adv. Mater.* **2010**, *22*, 2068; b) Y. Wang, F. Li, *Adv. Mater.* **2011**, *23*, 2134; c) Y. Wang, *Acc. Chem. Res.* **2016**, *49*, 1401.
- [11] A. Eichler-Volf, L. Xue, G. Dornberg, H. Chen, A. Kovalev, D. Enke, Y. Wang, E. V. Gorb, S. N. Gorb, M. Steinhart, *ACS Appl. Mater. Interfaces* **2016**, *8*, 22593.
- [12] a) Y. Wang, U. Gösele, M. Steinhart, *Nano Lett.* **2008**, *8*, 3548; b) Y. Wang, Y. Qin, A. Berger, E. Yau, C. He, L. Zhang, U. Gösele, M. Knez, M. Steinhart, *Adv. Mater.* **2009**, *21*, 2763; c) Y. Wang, L. Tong, M. Steinhart, *ACS Nano* **2011**, *5*, 1928.
- [13] R. Kumar, A. Bonicelli, S. Sekula-Neuner, A. C. B. Cato, M. Hirtz, H. Fuchs, *Small* **2016**, *12*, 5330.
- [14] D. J. Eichelsdoerfer, K. A. Brown, M. X. Wang, C. A. Mirkin, *J. Phys. Chem. B* **2013**, *117*, 16363.
- [15] S. Ichilmann, K. Rücker, M. Haase, D. Enke, M. Steinhart, L. J. Xue, *Nanoscale* **2015**, *7*, 9185.
- [16] a) Z. J. Zheng, W. L. Daniel, L. R. Giam, F. W. Huo, A. J. Senesi, G. F. Zheng, C. A. Mirkin, *Angew. Chem., Int. Ed.* **2009**, *48*, 7626; b) F. Brinkmann, M. Hirtz, A. M. Greiner, M. Weschenfelder, B. Waterkotte, M. Bastmeyer, H. Fuchs, *Small* **2013**, *9*, 3265; c) R. Kumar, S. Weigel, R. Meyer, C. M. Niemeyer, H. Fuchs, M. Hirtz, *Chem. Commun.* **2016**, *52*, 12310; d) C. Carbonell, D. J. Valles, A. M. Wong, M. W. Tsui, M. Niang, A. B. Braunschweig, *Chem* **2018**, *4*, 857.
- [17] P. A. Penttilä, S. Vierros, K. Utriainen, N. Carl, L. Rautkari, M. Sammalkorpi, M. Österberg, *Langmuir* **2019**, *35*, 8373.
- [18] K. H. Kang, H. C. Lim, H. W. Lee, S. J. Lee, *Phys. Fluids* **2013**, *25*, 042001.
- [19] R. D. Deegan, O. Bakajin, T. F. Dupont, G. Huber, S. R. Nagel, T. A. Witten, *Nature* **1997**, *389*, 827.